FATIGUE LIFE OF RAILWAY WHEELS UNDER THERMOMECHANICAL LOADS

A. Martín Meizoso, J. Gómez Jiménez, J.M. Rodríguez Ibabe and J. Gil Sevillano (*)

A computer program (TERMAL) has been developed to study crack propagation on railroad wheel rims. Current theories on fatigue crack propagation and fracture together with experimental data of wheel material properties have been used.

The program accounts for the effect of statical loads arising from residual stresses and of alternating loads imposed by contact. TERMAL starts with an assumed preexistant small defect on the rolling contact surface and, basically, calculates the LIFE OF THE WHEEL.

INTRODUCTION

A computer program (TERMAL) has been developed to study crack propagation on railroad wheel rims. Current theories on fatigue crack propagation and fracture together with experimental data of wheel material properties have been used.

The problem accounts for the effect of statical loads arising from residual stresses generated after braking action (calculated through an elasto-plastic finite element program) and of alternating loads imposed by the contact stresses developed under the rail-wheel contact. TERMAL starts with an assumed preexistant small defect on the rolling contact surface and, basically, calculates the LIFE OF THE WHEEL, conventionally taken as the number of cycles -wheel revolutions- that the wheel will withstand before the crack reaches the external side of the rim.

Related work has been previously published by Wetenkamp et al. (1), Wetenkamp and Kipp (2), Carter and Caton (3), Carter et al. (4), Kipp (5) and Nishioka et al. (6, 7).

RESIDUAL STRESSES

An independent elasto-plastic FEM program (8, 9) calculates the stresses thermally induced by a braking action. The program accounts for the temperature dependence of plastic flow curves in the full temperature range reached in the wheel. Fig. 1 shows

---

* Escuela Superior de Ingenieros Industriales (Universidad de Navarra), San Sebastián, Urdaneta, 7, SPAIN.

the discretization of the wheel and the locations of the heat source (brake shoe) used in the following examples. Axysimetric isoparametric elements of 6 and 8 nodes are used.

CONTACT STRESSES

For a given wheel diameter, radius of the rail, coeficient of friction and axle load, the ellipse of contact and pressure distribution on contact area are computed according to Hertz (10,11) (Timoshenko and Goodier (12), Saada (13)).

In order to calculate the stress field inside the wheel, the contact load distribution is discretizised into punctual loads. Stresses generated by each punctual load in a perfectly elastic semi-infinite solid are solved according to Boussinesq (14) or Cerruti (Saada (13)) for the normal and tangential load component, respectively. Superposition and Saint Venant principles make possible to compute stresses at distances longer than the punctual load spacing.

Shear stresses, promoting crack propagation modes II and III, have been neglected because they are approximately one order of magnitude smaller than normal stresses and usually appear asociated with strong normal compressive stresses.

Fig. 2 represents the s(zz) stress component for 120 MN wheel load. As it can be seen, s(zz) tensile stresses are quite small in comparison with compressive ones in the absence of friction. Tensile stresses are consequently not considered into the following calculations.

With a conservative aim, the maximum stress range is assumed to be applied at each depth, indepently of the actual contact location relative to the third dimension.

Furthermore, an approximate plastic correction has been made. The circunferential s(zz) stress is kept below the yield stress in any point. To maintain equilibrium conditions, contact stresses are moved to a deeper position. (displaced an amount equal to the plastified depth). Fig. 3 shows maximum and minimum s(zz) values as function of the depth, x.

STATIC AND ALTERNATING STRESS FIELDS

By "static (*) field" we will understand the maximum tensile field resultant of superposition of residual and contact stresses. Since tensile contact stresses generated by contact were neglected, the "static field" coincides with the residual stress field.

(*) In the sense that it decides static mode crack propagation and arrest, as opposed to (dynamic) fatigue propagation.

The effective alternating field, as only tensile stresses are assumed to induce fatigue crack growth, should coincide with the static field up to a certain depth, beyond which it should be identical to the contact one.

HYPOTHESIS AND METHODS OF CALCULATION

Three-dimensional stress configurations whose stress intensity factors are available apply only to circular or elliptical cracks. So, semicircular or semielliptical radial cracks emanating from the rim surface will only be considered.

Even if the initial crack starts with such a shape, its geometry is altered by the dissimilar growth of its front points under the complex stress field. Accordingly, some crack remodelling must be made after each growth step, as indicated below, to maintain a tractable geometry.

The maximum tensile residual stresses are developed into the wheel rim after cooling to ambient temperature (Wetenkamp, et al. (1). van Swaay(15)). Those are the residual stresses used for life calculations.

Stress intensity factors are calculated making use of the superposition principle.

Fatigue propagation and checks for unstable failure and arrest are calculated making use of both experimentally measured room-temperature crack growth rate and toughness data of wheel material.

Stress field components

In order to apply the superposition principle, it is necessary to calculate the normal stress distribution in the uncracked solid on the location of the crack plane. As it is well known, the stress intensity factor is then calculated on the basis of the stress distribution of oppossite sign acting on the surface of the crack.

For the reference system described in Fig. 4, the coordinates of the crack front are,

$$\begin{aligned} x &= a.\cos\psi \\ y &= c.\sin\psi \end{aligned} \qquad (1)$$

The normal static and alternating stress fields on the crack plane location in the uncracked body are calculated as referred above. The bidimensional heterogeneous stress distribution obtained is replaced by a second degree polynomial,

$$s = s1+s2.x+s3.y+s4.x^2+s5.x.y+s6.y^2 \qquad (2)$$

derived by a least-squares fitting made on the crack plane, covering up to the close neighbourhood beyond the crack front.

The points used for the fitting are the nodes of the FEM program developed for the thermo-elasto-plastic problem. A minimum of ten nodes are considered even for the samllest crack.

Stress intensity factors. Free surface correction

Mode I stress intensity factors for each point of the crack front are calculated according to the equations proposed by Shah and Kobayashi (16) for elliptical cracks in an infinite solid, with a correction for free surface effects. These equations allow to calculate stress intensity factors for pressure distribution on the crack faces,

$$p(x,y) = \sum_{i,j=0}^{3} A(i,j).x^i.y^j \qquad (3)$$

In our case, because of the approximation of the stress distribution by a second order polynomial, only the stress intensity factors corresponding to the terms of the development up to a second degree have been retained.

$$s1=1, \quad s2=x, \quad s3=y, \quad s4=x^2, \quad s5=x.y, \quad s6=y^2 \qquad (4)$$

Those factors, $K(s(i))/s(i) = mf(i)$ $i=1,\ldots,6$, are handled separately to allow for a different free surface effect correction for each term.

The problem of the free surface correction in the semi-infinite solid has been tackled by Newman and Raju (17) for a uniform pressure distribution in a<c cracks. Thus, the K(s(1))term of Shah and Kobayashi has been replaced by that of Newman and Raju's. Correction factors for the other terms are not available and a generic 1.06 factor has been employed for all of them. It represents the mid point between the value for internal cracks (lower bound, 1) and the value for through the thickness bidimensional cracks (upper bound, 1.12). Those two extreme values are also used for estimating fatigue life upper and lower bounds.

Fatigue

Once the stress intensity factor range for each point of the crack front is computed, the crack advances by displacing its front points a distance computed from direct application of Paris law (Paris and Erdogan (18)). Points with $\Delta K < \Delta Kth$ (fatigue thershold) remain unchanged. Displacements are assumed orthogonal to the crack front (Tian, Lu and Zhu (19)).

Since fields and crack geometry will vary along the wheel rim, it is convenient to use small crack advance increments in the computation steps. In this particular case a step range from 1 to 2% of the mean size has been found to be most convenient for life predictions.

Crack remodelling

To be able to compute stress intensity factors for the new crack front, an ellipse centered on the free surface is fitted to the new points.

For each step of crack propagation, upper and lower bounds are computed assuming two more ellipses (former semiaxes plus or minus twice their standard deviation, calculated from the deviation of the real points relative to the remodelled crack front). Also 1.12 and 1.00 are taken as extreme values of the free surface effect factor in these calculations.

End of life

Two possible end of life circunstances are considered:

1. WEAR: Once the estimated total number of cycles for inacceptable wear of the flange is achieved ($5\ 10^7$ cycles).

2. FRACTURE: Once the crack reaches the external side of the rim.

   At this moment, geometric hypothesis used into the K calculations become unvalid. Furthermore, the remaining life once the crack reaches the wheel side is considered marginal for life predictions.

Flow charts

Figure 5 shows a general scheme of the program flow chart: the fundamental steps in computational procedure and considered conditions for changing from a propagation mode to another one.

EXAMPLE OF RESULTS

As an example of the program capabilities, the life prediction for a new flat plate, 1250 mm Ø, surface treated, UIC R-7 grade (20) wheel is presented.

Four different braking application conditions are studied: 90 Kw for 15 minutes, 60, 55 and 50 Kw for 30 minutes. In every case, correct and incorrect brake shoe location are studied (centered on the rolling surface and partly applied over the rim) as indicated in fig.1. The wheel is later allowed to cool up to room temperature, in order to compute residual stresses.

The cases considered are:

CASE 0.-	90 Kw	for	15 mn.,	centered	shoes	(correct)
CASE 1.-	60 Kw	"	30	centered	"	
CASE 2.-	60 Kw	"	30	over the rim	",	(incorrect)
CASE 3.-	55 Kw	"	30	centered	"	

CASE 4.- 55 Kw for 30 mn., over the rim shoes (incorrect)
CASE 5.- 50 Kw " 30 centered "
CASE 6.- 50 Kw " 30 over the rim "

Figures 6-11 correspond to CASE 0. Figures 12-13, to CASE 2. Figure 14 shows a limit curve (estimated) for braking practice with this particular wheel.

Tables 1 and 2 show the maximum non-propagating defects and predicted life for every case studied.

ACKNOWLEDGEMENTS

The TERMAL program has been developed as part of a research project in cooperation with CAF (Construcciones y Auxiliar de Ferrocarriles S.A., Spain), with the sponsorship of the "Comisión Asesora de Investigación Científica y Técnica", Acción Concertada no. 7/79.

LIST OF SYMBOLS

a,c = ellipse semiaxes (mm).
A = coefficients of polynomial pressure distribution.
K = stress intensity factor (MPa $\sqrt{m}$)
mf = K/s for each stress component ($\sqrt{m}$)
p = internal pressure distribution (MPa).
s = normal stress (MPa).
s1,s2,... = components of the normal stress (MPa).
x,y = elliptical angle (rad).

REFERENCES

1. Wetenkamp, H.R., Sidebottom, D.M. and Schrader, H.J., "The Effect of Brake Shoe Action on Thermal Cracking and on Failure of Wrought Steel Railway Car Wheels", University of Illinois Bulletin, 47, 1950.

2. Wetenkamp, H.R. and Kipp, R.M., "Safe Thermal Loads for a 33 inch. Railroad Wheel", Griffin Wheel Company, 1975.

3. Carter, C.S. and Caton, R.G., "Fracture Resistance of Railroad Wheels", Boeing Commercial Airplane Company, PB 243 638, 1974.

4. Carter, C.S., Caton, R.G. and Guthrie, J.L. "Fracture Resistance and Fatigue Crack Growth Characteristics of Railroad Wheels and Axles", Boeing Commercial Airplane Company, PB 298 312, 1977.

5. Kipp, R.M., "Investigations of Crack Growth in Railroad Car Wheels Caused by Thermally Induced Residual Stress Changes and Cyclic Mechanical Loading", Dept. of Theoretical and Applied Mechanics, Univ. Illinois, T. & A.M. Report no. 428, 1978.

6. Nishioka, K., Nishimura, S., Hirakawa, K., Tokimasa, K. and Suzuki, S., "Fracture Mechanics Approach to the Strength of Wheelsets", 6th. Int. Wheelset Congress, Colorado Springs, 1, pp. 2.4.1.-15, 1978.

7. Nishioka, K., Hirakawa, K., Sakamoto, H., Toyama, K., Suzuki, S. and Hamasaki, A., "Development of Improved Railroad Wheels", 7th. Int. Wheelset Congress, Viena, pp. 6.1-14, 1981.

8. Egaña, J.M., Giménez, J.G., "Estudio Elastoplástico de Sólidos de Revolución Sometidos a Cargas Térmicas", 4'Congreso Nacional sobre la Teoría de Mecanismos y Máquinas, Valencia, D.6.1-15, 1981.

9. Egaña, J.M., Giménez, J.G., "Analysis by the Finite Element Method of Thermoplastic Problems in Axisymmetrical Solids", to be published.

10. Hertz, H., J. Math., 92, 1881. Quoted by Timoshenko (12).

11. Hertz, H., "Gesammelte Werke", 1, pp. 155, Leipzig, 1895.

12. Timoshenko, S. and Goodier, J.N., "Theory of Elasticity", McGraw-Hill, New York, 1951.

13. Saada, A.S., "Elasticity, Theory and Applications", Pergamon, Oxford, 1974.

14. Boussinesq, J., "Application des potentiels (...)", Paris, 1885. Quoted by Saada (13).

15. Van Swaay, J.L., "The Mechanism of Thermal Cracking in Railway Wheels", 3rd. Int. Wheelset Congress, Shefield, pp. 8/1-8, 1969.

16. Shah, R.C. and Kobayashi, A.S. "Stress Intensity Factor for an Elliptical Crack Under Arbitrary Normal Loading", Eng. Fract. Mech., 3, pp. 71-96, 1971.

17. Newman, J.C. and Raju, I.S., "An Empirical Stress-Intensity Factor Equation for the Surface Crack", Eng. Fract. Mech. 15, pp. 185-192, 1981.

18. Paris, P.C. and Erdogan, F., "A Critical Analysis of Crack Propagation Laws", J. Basic Eng., Trans.ASME, 85, pp. 528-534,1963.

19. De-Chang Tian, Da-Quan Lu and Jia-Ju Zhu, "Crack Propagation Under Combined Stresses in Three-Dimensional Medium", Eng. Fract. Mech., 16, pp. 5-17, 1982.

20. Union Internationale des Chemins de Fer (U.I.C.), "Specification Technique pour la Fourniture de Roues

Monoblocs en Acier non Allié, Laminé et Moulé pur Materiel Roulant, Moteur et Remorqué", 812-3 0, 4'ed., pp. 1.35, 1974.

TABLE 1.- Maximum radius for non-propagating defects (mm).

	CASE NO						
NODE	0	1	2	3	4	5	6
16	2.00	5.15	0.75	-	0.70	-	3.04
17	0.66	1.44	0.68	9.64*	0.69	-	2.59
18	0.45	0.78	0.64	4.22*	0.66	-	2.47
19	0.42	0.67	0.62	2.67*	0.72	-	3.53
20	0.40	0.64	0.61	2.32*	0.82	-	5.69
21	0.39	0.65	0.62	2.25*	1.15	-	9.83
22	0.39	0.67	0.75	2.59*	2.52	-	-
23	0.41	0.77	2.32	4.09*	7.59	-	-
24	0.50	1.17	8.38	9.35*	-	-	-
25	0.86	2.54	-	-	-	-	-
26	3.82	7.82	-	-	-	-	-

* arrest.

TABLE 2.- Life predictions.

CASE NO.	inicial defect	Life	
		cycles	Kms
0	.5x.5	2,500,000	10,000
1	.7x.7	4,700,000	18,000
2	.7x.7	2,800,000	11,000
3	4x4	∞	∞
4	1x1	4,900,000	19,000
5	-	∞	∞
6	10x10	15,000,000	59,000

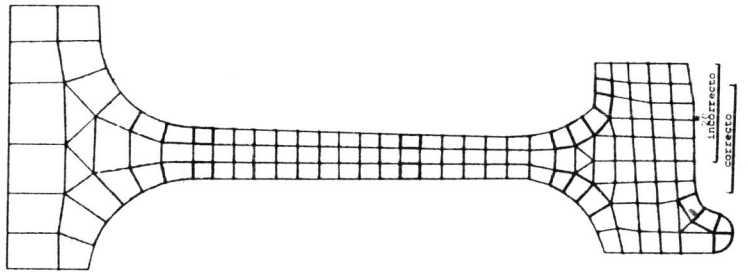

Fig. 1: Discretization of a new, flat plate, 1250 mm Ø railroad wheel.

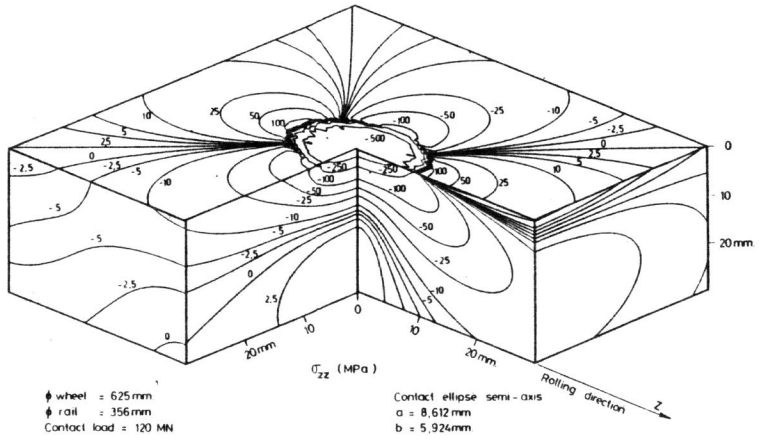

Fig. 2: s(zz) wheel-rail contact stress component inside the wheel.

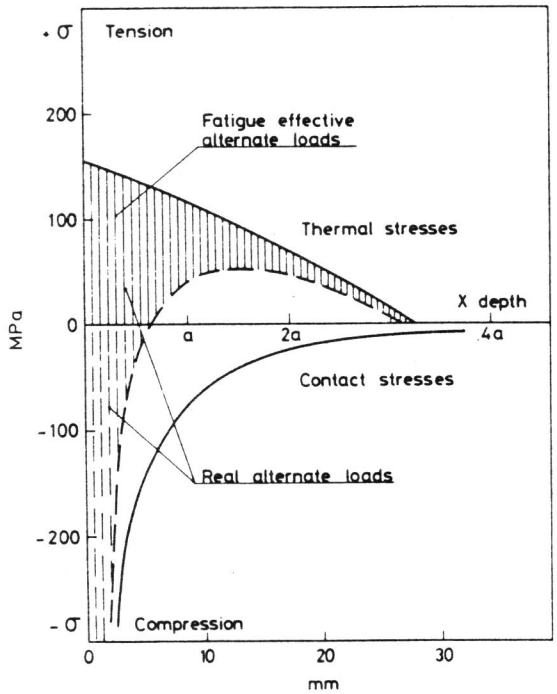

Fig. 3: s(zz) range as a function of the depth.

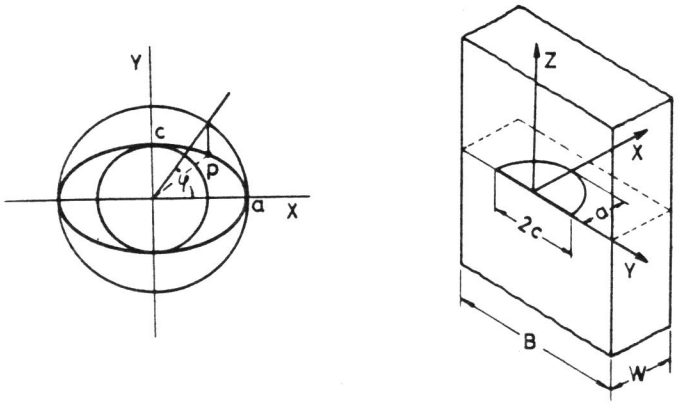

Fig. 4: Reference system.

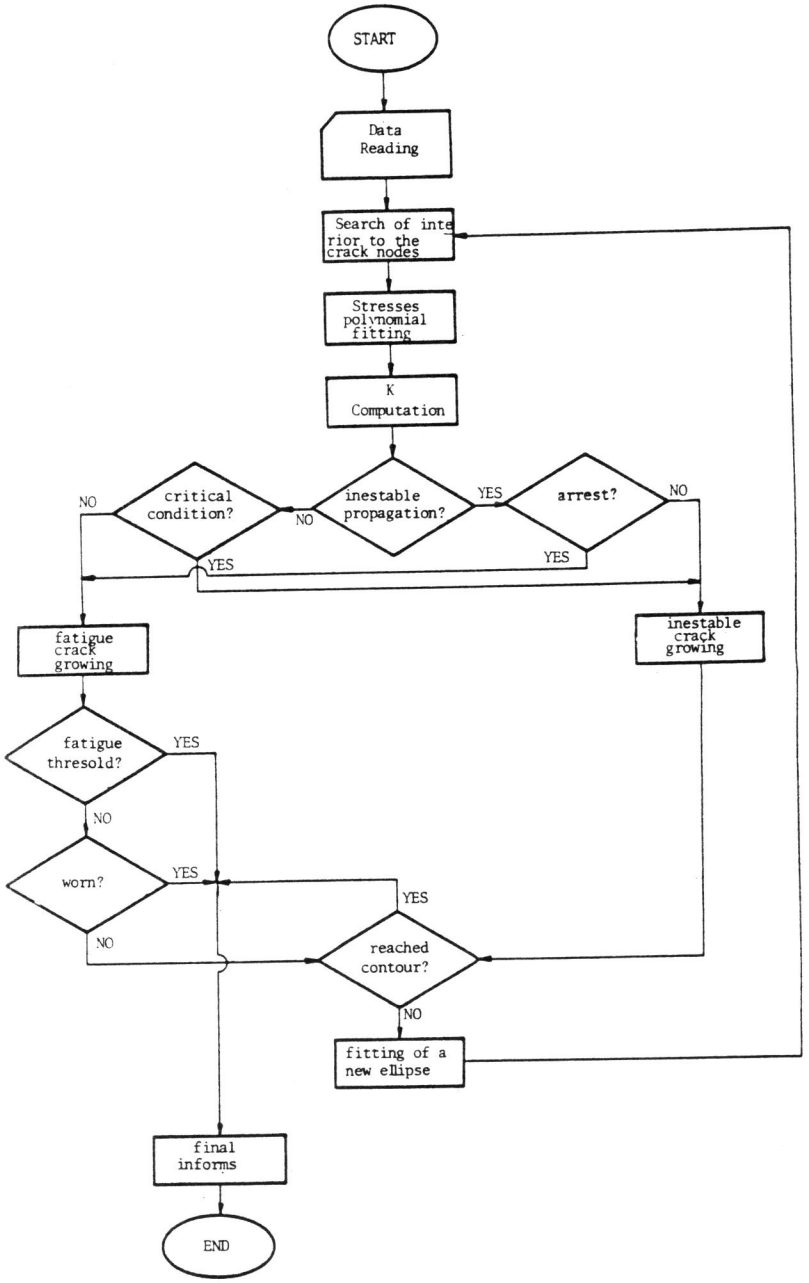

Fig. 5: General scheme of the program flow chart.

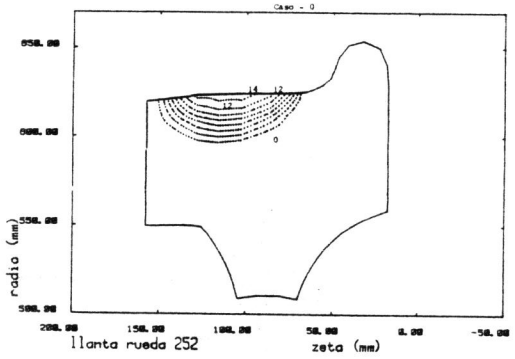

Fig. 6: Isostress σ_{zz} (MPa)

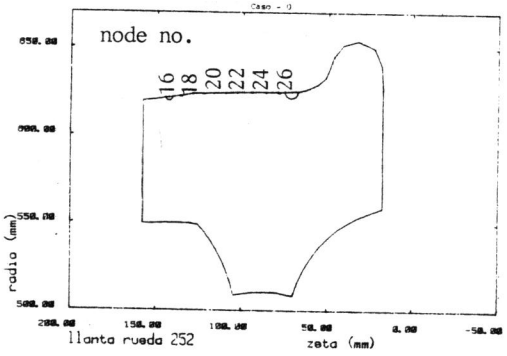

Fig. 7: Non-propagating defects

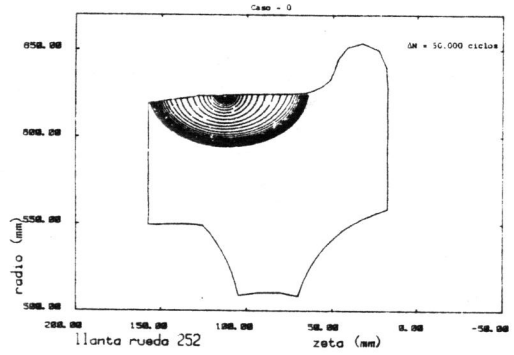

Fig. 8: Successive crack fronts

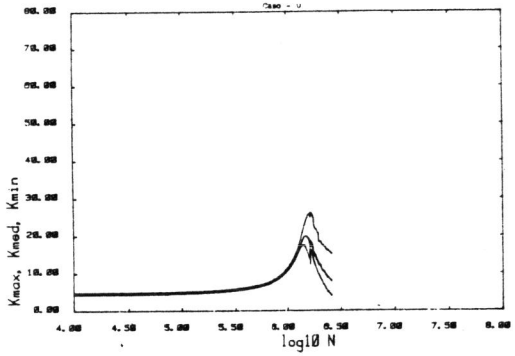

Fig. 9: K range along crack front. (MPa $\sqrt{m}$)

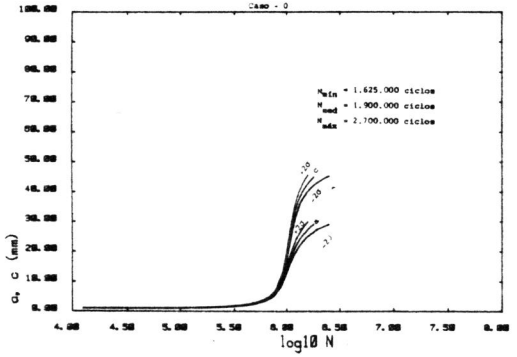

Fig. 10: Semiaxes evolution and 2σ confidence limits for fatigue propagation

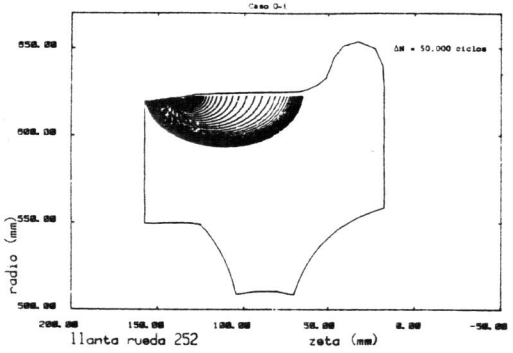

Fig. 11: Successive crack fronts

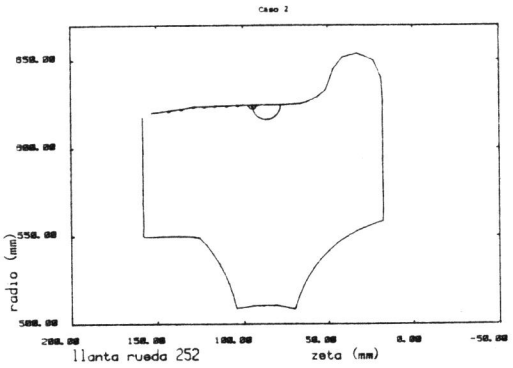

Fig. 12: Non-propagating defects

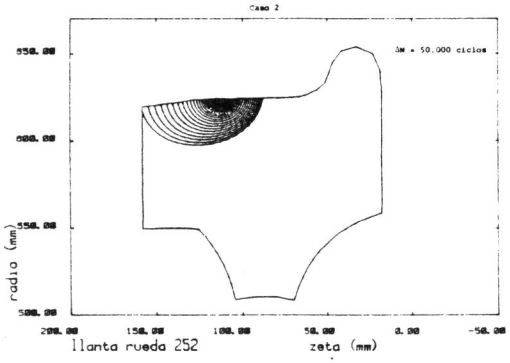

Fig. 13: Successive crack fronts

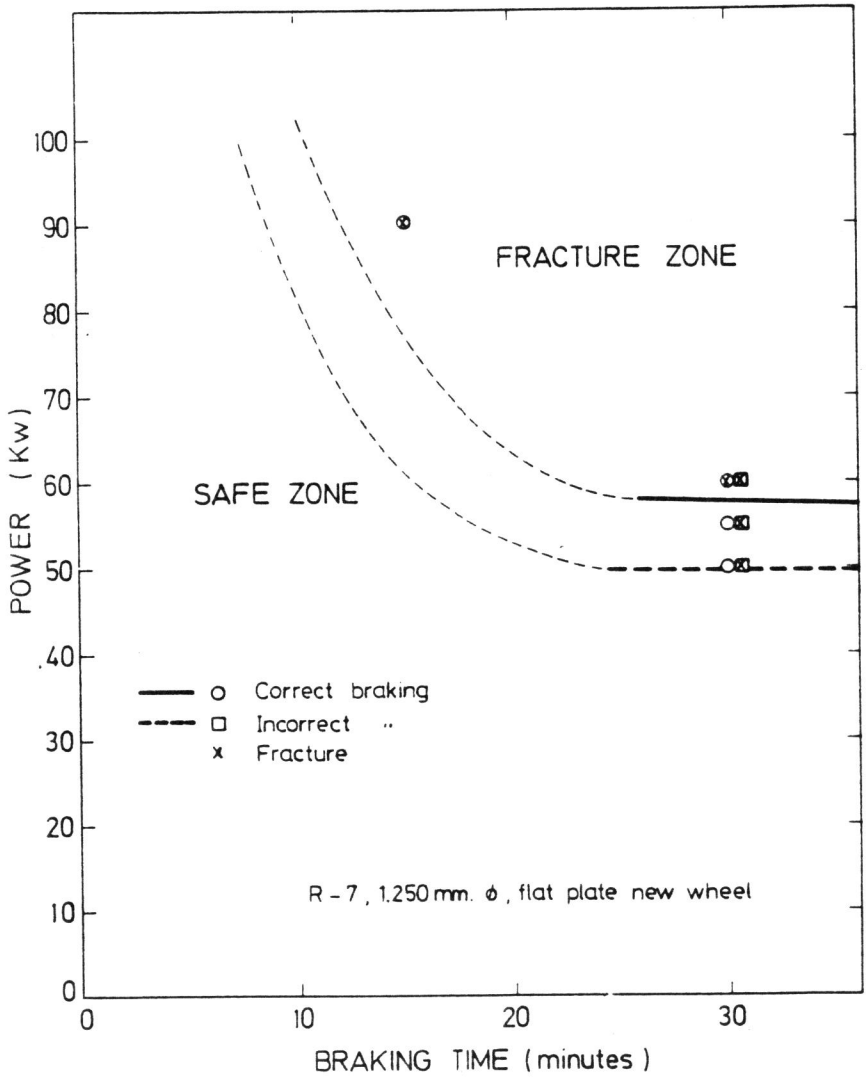

Fig. 14: Limit curve (estimated) for braking action.